Presented at the First International Conference on Pressure Vessel Technology Oct., 1969. Holland.

(9) (12)

II—61

On the Prediction of Failure in Pressurized Vessels

E. S. FOLIAS
University of Utah
Salt Lake City, Utah

ABSTRACT

This report discusses a fracture criterion for the prediction of failure in flawed pressurized vessels of arbitrary shape. A comparison with some of the existing experimental data in the literature substantiates its potential use.

NOMENCLATURE

c	half crack length
D	flexural rigidity $\left(Eh^3/\left[12(1-\nu^2)\right]\right)$
E	Young's modulus
G	shear modulus
h	thickness
k	fracture toughness (for flat sheets)
J, I	coefficients as defined in text
q_0	uniform internal pressure
R	radius of the shell
γ^*	surface energy per unit area
λ^4	$\dfrac{Ehc^4}{R^2D}\left(\equiv\dfrac{12(1-\nu^2)c^4}{R^2h^2}\right)$
λ_j	$\dfrac{Ehc^4}{R_j^2D}$ $(j = 1, 2, 3, x, y)$
ν	Poisson's ratio
π	3.14
σ_Y	uniaxial yield stress
σ_{YB}	biaxial yield stress
σ_u	ultimate tensile stress (for a flat sheet)
σ^*	$\dfrac{\sigma_Y + \dfrac{\sigma_Y+\sigma_u}{2}}{2}$
σ_h	hoop stress
$\overline{\sigma}^{(e)}, \overline{\sigma}^{(b)}, \overline{\tau}$	applied to the crack stress components

INTRODUCTION

It is well known [1-5] that initially curved sheets containing throughcracks present a reduced resistance to fracture initiation. Consequently, the presence of a crack in the walls of a pressure vessel can severely reduce the strength of the structure and can cause sudden failure at nominal tensile stresses less than the material yield strength. Therefore, to ensure the integrity of a structure, the designer must have cognizance of the relation between fracture load, flaw shape and size, and structural geometry.

Such a relation has been derived by the author; and, for cylindrical and spherical pressure vessels, the results are reported in Ref. [6]. In this paper the author, in view of some recent developments [5],

Table 1.

Long cylinder axial crack

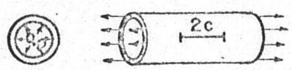

$$I = 1 + \frac{5\pi}{64}\lambda^2$$

$$J \approx 0$$

$$\bar{\sigma}^{(e)} = \sigma_h = q_o R/h$$

Long cylinder peripheral crack

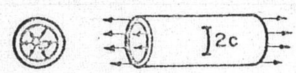

$$I = 1 + \frac{\pi\lambda^2}{64}$$

$$J \approx 0$$

$$\bar{\sigma}^{(e)} = \frac{\sigma_h}{2} = q_o R/2h$$

Spherical cap

$$I = 1 + \frac{3\pi\lambda^2}{32}$$

$$J \approx 0$$

$$\bar{\sigma}^{(e)} = \sigma_h = q_o R/2h$$

Conical circular

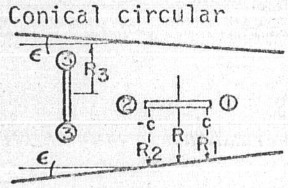

$$I_{①} = 1 + \frac{5\pi}{64}\lambda_1^2$$

$$I_{②} = 1 + \frac{5\pi}{64}\lambda_2^2$$

$$I_{③} = 1 + \frac{\pi}{64}\lambda_3^2$$

$$J \approx 0$$

$R_1 = R - c \tan \epsilon$

$R_2 = R + c \tan \epsilon$

Toroidal

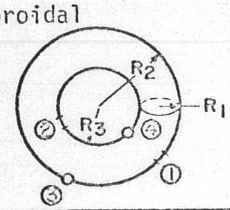

$$I_{①} = 1 + \frac{5\pi}{64}\lambda_1^2 + \frac{\pi}{64}\lambda_2^2$$

$$I_{②} = 1 + \frac{5\pi}{64}\lambda_1^2 - \frac{\pi}{64}\lambda_3^2$$

$$I_{③} = 1 + \frac{5\pi}{64}\lambda_2^2 + \frac{\pi}{64}\lambda_1^2$$

$$I_{④} = 1 - \frac{5\pi}{64}\lambda_3^2 + \frac{\pi}{64}\lambda_1^2$$

$J \approx 0$

o - indicates cracks normal to the paper

Arbitrary Geometry

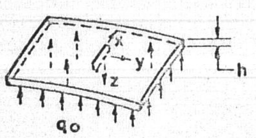

$$I = 1 + \frac{\pi\lambda_x^2}{64} + \frac{5\pi\lambda_y^2}{64}$$

$$J \approx 0$$

(where we assumed $\bar{\sigma}^{(b)} = \bar{\tau} = 0$.)

*The expressions in this table are valid for $\lambda \leq 1$ only. For larger values of λ, see Refs. [5] and [6].

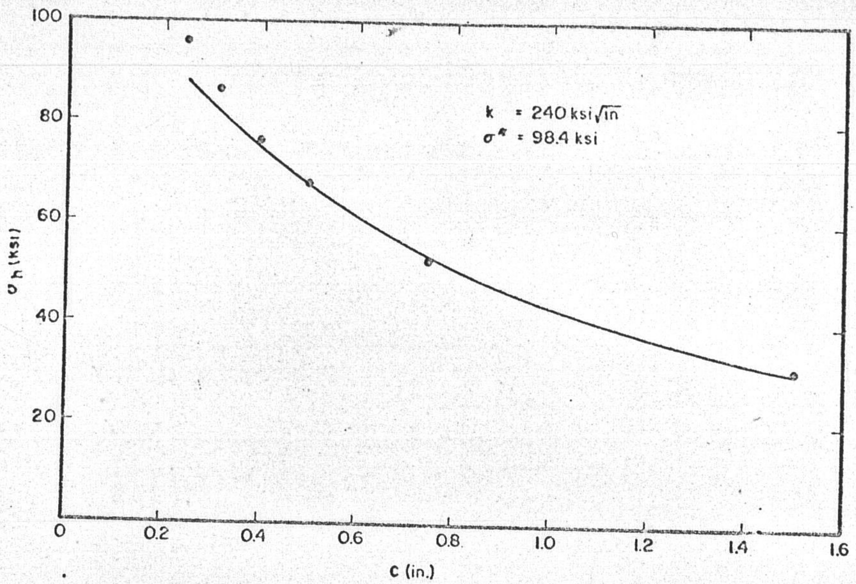

FIG. 1 COMPARISON BETWEEN THEORY AND EXPERIMENT FOR 30 PERCENT ZIRCALOY-2 N-REACTOR TUBES WITH V-SHAPE CRACKS

generalizes his fracture criterion to include other shell geometries and compares his theoretical results with the experimental data existing in the literature.

FRACTURE CRITERION

In deriving a fracture criterion two ingredients are necessary: (1) the stress distribution due to the presence of the crack and (2) an energy balance for crack initiation. Such a criterion incorporating correction factors for geometry and plasticity effects has been derived by the author. The details are given in Ref. [6], and an outline of the derivation is given in the Appendix. The criterion reads[1]

$$\bar{\sigma}^{(e)} \left\{ \frac{(33+6\nu-7\nu^2)(1+\nu)}{3(9-7\nu)} J^2 + I^2 \right\}^{\frac{1}{2}} = \frac{2\sigma^*}{\pi} \cos^{-1}\left[\exp\left(-\frac{\pi k^2}{8\sigma^{*2}c}\right)\right] \quad (1)$$

where the coefficients I and J are functions of the parameter λ and are given in Table 1.

By Eq. (1) one would expect, therefore, to predict failure in pressurized vessels containing through-the-thickness cracks. Inasmuch as theory in general is not useful unless there exists experimental evidence to support it, in the next few pages we will compare our results with some of the experimental data existing in the literature.

In order to utilize Eq. (1), however, one must know a priori the fracture toughness k. This difficulty can be eliminated if one proceeds in the following manner: (1) use the test data and compute the k's, (2) find the average k, and (3) use the k_{av} to predict failing hoop stresses.[2]

EXPERIMENTAL DATA[2]

R. C. Aungst's study[3] shows results of tests on 2.7-in. diameter, 0.26-in. thick N-reactor tube with v-shape cracks under the following conditions:

Material: 30 percent cold drawn zircaloy-2.

σ_Y: 98 ksi	$\sigma^* =$ 98.4 ksi
σ_u: 98.6 ksi	$k =$ 240 ksi $\sqrt{\text{in.}}$

[1] The analysis was based on thin shallow shell theory; therefore, Eq. (1) is valid only for $(h/R) \leq 0.01$ and $(L/R) \leq 0.1$, where L is a linear dimension

[2] See Ref. [7].

[3] R. C. Aungst, "Additional Crack Propagation Tests on Zircaloy-2 Pressure Tubes," *Electrotechnical Technology*, vol. 4, no. 7-8, July/August 1966.

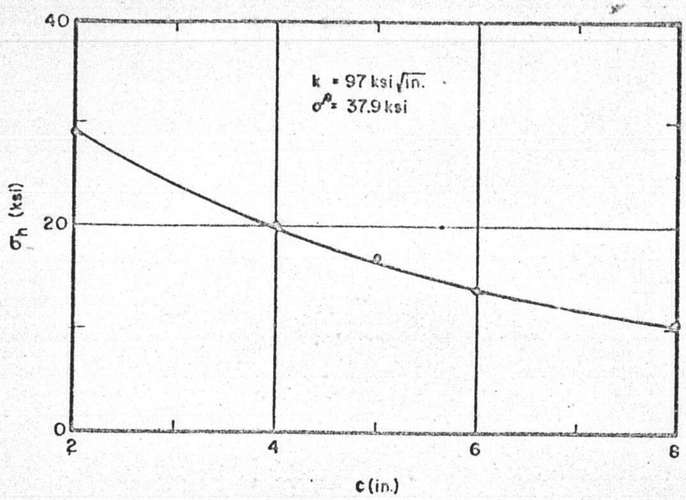

FIG. 2 COMPARISON BETWEEN THEORY AND EXPERIMENT FOR ABS-B STEEL SPHERICAL VESSELS

$T°$ C	c (in.)	λ	I	σ_h exp. ksi	σ_h calc. ksi
25	0.250	0.76	1.12	96.0	88.2
25	0.315	0.96	1.20	86.2	81.8
25	0.405	1.23	1.28	76.5	77.1
25	0.500	1.53	1.40	67.6	70.0
25	0.750	2.28	1.75	52.4	53.5
25	1.500	4.57	2.89	31.4	29.5

The results are plotted in Fig. 1. Notice that the agreement is very good for large crack lengths. However, for small crack lengths the predicted values are somewhat lower. This is not contrary to our expectations for our calculations were based on through the thickness cracks.

Sopher et al.[4] give results of tests on 9-ft diameter, 3-in. thick spheres with full-thickness cracks under the following conditions:

Material: ABS-B Steel

σ_Y: 30.7 ksi $\sigma^* = 37.9$ ksi

σ_u: 59.4 ksi $k = 102$ ksi $\sqrt{\text{in.}}$

[4] R. P. Sopher, A. L. Lowe, D. C. Martin, and P. J. Rieppel, "Evaluation of Weld Joint Flaws on Initiating Points of Brittle Fracture," *Welding J.*, November 1959, p. 441S.

[5] R. B. Anderson and T. L. Sullivan, "Fracture Mechanics of Through-Cracked Cylindrical Pressure Vessels," *NASA TN D-3252*.

$T°$ F	c (in.)	λ	I	σ_h exp. ksi	σ_h calc. ksi
40	2	0.57	1.13	28.15	28.4
40	2	0.57	1.13	28.15	28.4
40	4	1.14	1.29	19.70	19.8
40	5	1.42	1.40	16.90	16.8
40	6	1.70	1.55	13.10	14.0
40	8	2.27	1.85	11.20	10.3

The results are plotted in Fig. 2. The agreement is very good.

Anderson and Sullivan[5] show results of tests on 6-in. diameter, 0.060-in. thick cylinders with full-thickness cracks under the following conditions:

(1) Material: 2014-T6A1

σ_Y: 90.5 ksi $\sigma^* = 91.9$ ksi

σ_u: 93.9 ksi $k = 51.6$ ksi $\sqrt{\text{in.}}$

$T°$ F	c (in.)	λ	I	σ_h exp. ksi	σ_h calc. ksi
–423°	0.052	0.22	1.02	82.2	85.0
–423°	0.125	0.53	1.06	63.4	65.0
–423°	0.250	1.07	1.23	39.6	43.0
–423°	0.750	1.60	1.45	32.0	31.2
–423°	0.500	2.13	1.68	21.9	23.4
–423°	0.625	2.66	1.93	19.8	18.5
–423°	0.875	3.72	2.46	13.2	12.4
–423°	1.000	4.26	2.73	11.9	10.6

The results are plotted in Fig. 3. The agreement is good.

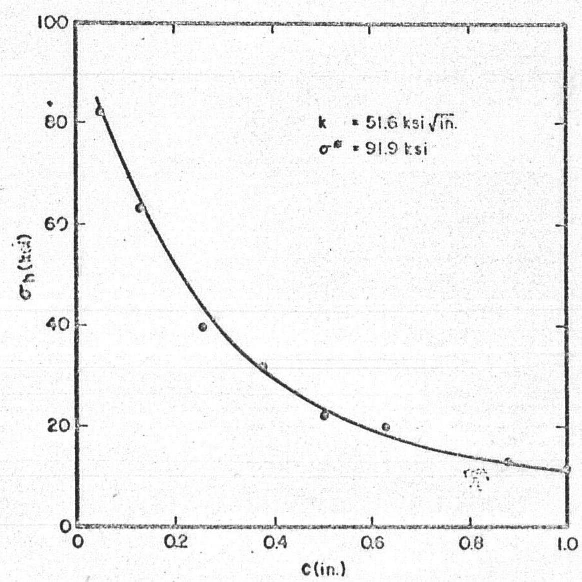

FIG. 3 COMPARISON BETWEEN THEORY AND EXPERIMENT FOR 2014-T6A1 CYLINDRICAL VESSELS AT –423° F

(2) Material: 2014-T6A1

σ_Y: 82.0 ksi $\sigma^* = 85.0$ ksi

σ_u: 93.9 ksi $k = 48.6$ ksi $\sqrt{\text{in.}}$

$T°$ F	c (in.)	λ	I	σ_h exp. ksi	σ_h calc. ksi
−320°	0.057	0.24	1.02	71.6	77.0
−320°	0.075	0.32	1.03	70.6	73.0
−320°	0.100	0.43	1.05	63.7	66.0
−320°	0.125	0.53	1.06	58.5	61.5
−320°	0.150	0.64	1.09	52.2	56.1
−320°	0.200	0.85	1.15	47.4	47.7
−320°	0.250	1.06	1.23	40.1	41.0
−320°	0.375	1.60	1.45	30.2	29.2
−320°	0.500	2.13	1.66	23.1	22.3
−320°	0.625	2.66	1.93	18.6	17.6
−320°	0.875	3.72	2.45	14.4	11.6
−320°	1.000	4.26	2.73	11.3	9.8

The results are plotted in Fig. 4. The agreement is good.

(3) Material: 2014-T6A1

σ_Y: 68.0 ksi $\sigma^* = 70.8$ ksi

σ_u: 79.0 ksi $k = 43.4$ ksi $\sqrt{\text{in.}}$

$T°$ F	c (in.)	λ	I	σ_h exp. ksi	σ_h calc. ksi
room	0.06	0.24	1.02	64.4	66.4
room	0.25	1.06	1.23	34.0	36.1
room	0.50	2.23	1.73	20.6	19.1
room	1.00	4.26	2.73	9.7	8.9

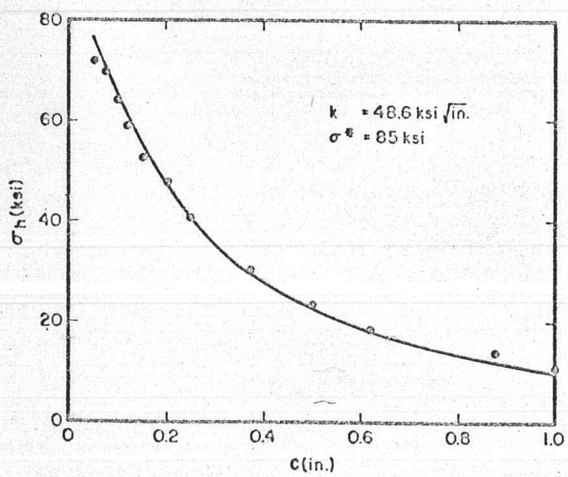

FIG. 4 COMPARISON BETWEEN THEORY AND EXPERIMENT FOR 2014-T6A1 CYLINDRICAL VESSELS AT −320°F

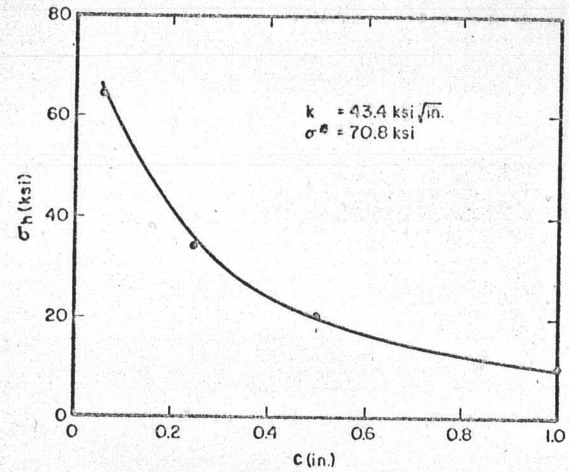

FIG. 5 COMPARISON BETWEEN THEORY AND EXPERIMENT FOR 2014-T6A1 CYLINDRICAL VESSELS AT ROOM TEMPERATURE

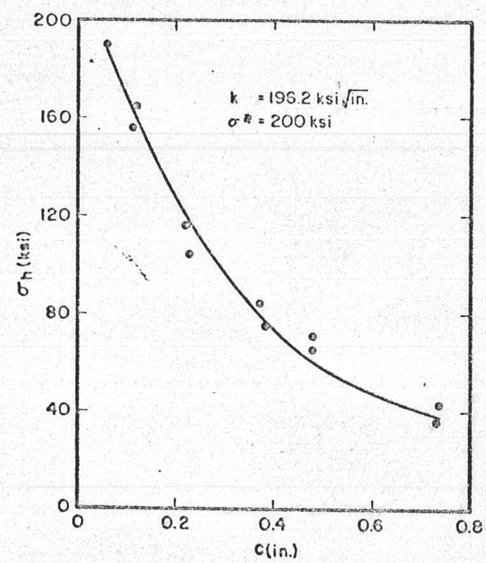

FIG. 6 COMPARISON BETWEEN THEORY AND EXPERIMENT FOR 5A1-2.5Sn-Ti CYLINDRICAL VESSELS AT −320°F

The results are plotted in Fig. 5. The agreement is good.

They also show results of tests on 6-in. diameter, 0.020-in. thick cylinders with full thickness cracks under these conditions:

Material: 5A1-2.5S_n−Ti

σ_{YB}: 222 ksi $\sigma^* = 200$ ksi

σ_u: not specified $k = 196$ ksi $\sqrt{\text{in.}}$

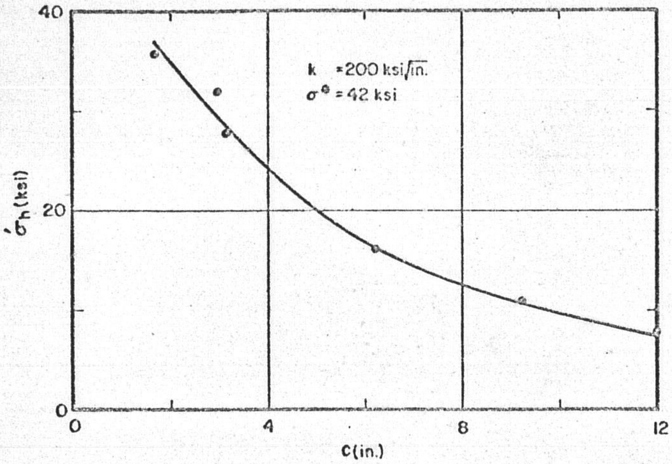

FIG. 7 COMPARISON BETWEEN THEORY AND EXPERIMENT FOR B.S. 1501-161: 1958, GRADE B SPHERICAL VESSELS

$T°$ F	c(in.)	λ	I	σ_h exp. ksi	σ_h calc. ksi
−320°	0.063	0.46	1.05	190.4	191
−320°	0.121	0.89	1.17	164.9	165
−320°	0.115	0.84	1.15	156.9	169
−320°	0.220	1.62	1.45	115.5	121
−320°	0.227	1.67	1.47	105.1	119
−320°	0.367	2.70	1.58	84.9	97
−320°	0.383	2.82	2.02	74.6	74
−320°	0.473	3.48	2.35	71.8	60
−320°	0.481	3.54	2.38	66.2	59
−320°	0.740	5.45	3.28	44.1	36
−320°	0.730	5.37	3.27	35.9	36

The results are plotted in Fig. 6. The agreement is fairly good. It should be pointed out that titanium alloys exhibit significant increase in biaxial yield strength relative to uniaxial yield strength. Hence, the von Mises yield criterion may or may not be applicable. However, if one uses a σ^* slightly less than 200 ksi, even better agreement is noticed.

Taylor and Burdekin[6] give results of tests on 58-in. diameter, 0.50-in. thick spheres with through-thickness cracks.

Material: B.S. 1501-161: 1958, Grade B
σ_Y: 36.0 ksi at 80° C $\sigma^* = 42.2$ ksi
σ_u: 60.9 ksi at 80° C $k = 200.0$ ksi $\sqrt{\text{in.}}$

T° C	c (in.)	λ	I	σ_h exp. ksi	σ_h calc. ksi
78	1.69	0.80	1.16	35.60	36.6
80	3.15	1.50	1.45	27.70	28.1
78	6.20	2.94	2.22	16.20	16.0
80	9.20	4.37	3.17	10.85	10.1
80	12.00	5.69	4.12	7.55	7.0
0-10	3.00	1.42	1.41	31.90	30.1

The results are plotted in Fig. 7. The agreement is good except at one point, but this is due to a temperature change.

Irvine, Quirk, and Bevitt[7] show results of tests on 5-ft diameter, 1-in. thick, cylindrical vessels with through cracks under the following conditions:

Material: 0.36 percent C Steel
σ_Y: 33 ksi $\sigma^* = 40$ ksi
σ_u: 61 ksi $k = 179$ ksi $\sqrt{\text{in.}}$

T	c (in.)	λ	I	σ_h exp. ksi	σ_h calc. ksi
	3	0.99	1.20	27.60	32.2
	3	0.99	1.20	30.00	32.2
	3	0.99	1.20	32.40	32.2
	6	1.98	1.61	18.80	20.8
	6	1.98	1.61	21.00	20.8
	12	3.96	2.58	9.65	10.2
	12	3.96	2.58	11.65	10.2
	12	3.96	2.58	13.00	10.2

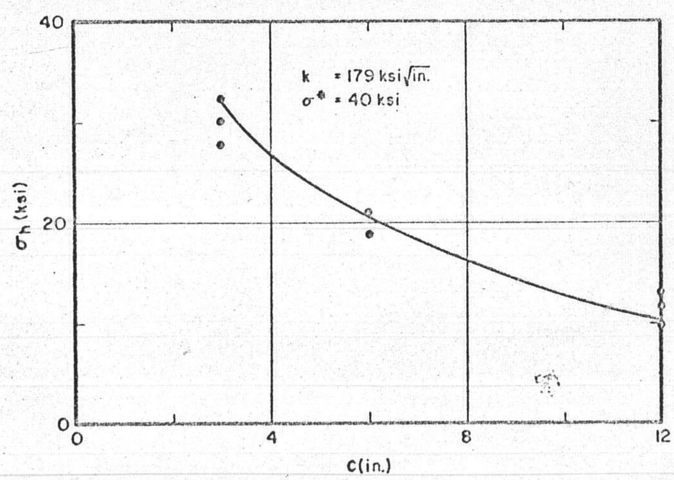

FIG. 8 COMPARISON BETWEEN THEORY AND EXPERIMENT FOR 0.36 PERCENT C STEEL CYLINDRICAL VESSELS

[6] T. E. Taylor and F. M. Burdekin, "Unstable Fracture by the Shear Mode in Spherical Vessels with Long Flaws," B.W.R.A. C157/2/66.

[7] W. H. Irvine, A. Quirk, and E. Bevitt, "Fast Fracture of Pressure Vessels: An Appraisal of Theoretical and Experimental Aspects and Application to Operational Safety," *J. Brit. Energy Soc.*, January 1964.

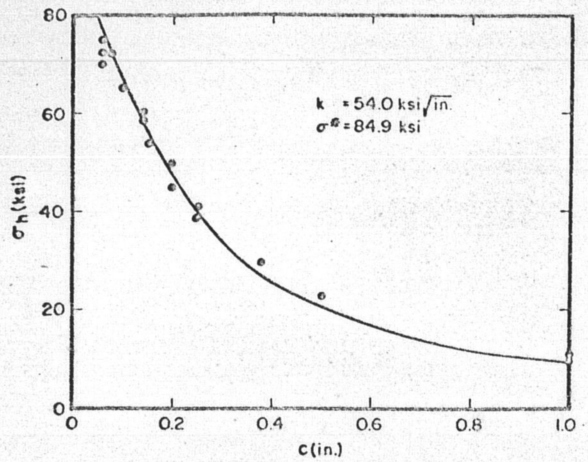

FIG. 9 COMPARISON BETWEEN THEORY AND EXPERIMENT FOR 2014-T6A1 CYLINDRICAL VESSELS AT –321°F

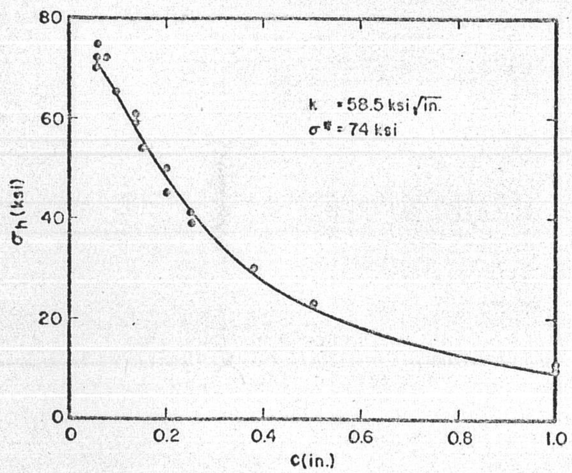

FIG. 10 COMPARISON BETWEEN THEORY AND EXPERIMENT FOR 2014-T6A1 CYLINDRICAL VESSELS AT –321°F

The results are plotted in Fig. 8. The agreement is fairly good.

Getz, Pierce and Calvert[8] give results of tests on 3-in. diameter, 0.060-in. thick cylindrical vessels with through-the-thickness cracks under the following conditions.

(1) Material: 2014-T6 aluminum alloy

σ_Y: 81.9 ksi $\quad\quad \sigma^* = 84.9$ ksi

σ_u: 93.9 ksi $\quad\quad k = 54.0$ ksi $\sqrt{\text{in.}}$

[8]D. L. Getz, W. S. Pierce, and H. F. Calvert, "Correlation of Uniaxial Notch Tensile Data with Pressure Vessel Fracture Characteristics," *ASME Paper 63-WA-187*.

T	c (in.)	λ	I	σ_h exp. ksi	σ_h calc. ksi
–321	0.060	0.36	1.03	70	79
–321	0.060	0.36	1.03	72	79
–321	0.060	0.36	1.03	75	79
–321	0.075	0.45	1.05	72	74
–321	0.100	0.60	1.08	65	67
–321	0.140	0.84	1.15	60	59
–321	0.140	0.84	1.15	59	59
–321	0.150	0.90	1.17	54	56
–321	0.200	1.20	1.28	45	47
–321	0.200	1.20	1.28	50	47
–321	0.250	1.50	1.40	39	39
–321	0.250	1.50	1.40	41	39
–321	0.375	2.25	1.73	30	27
–321	0.375	2.25	1.73	30	27
–321	0.500	3.00	2.11	23	20
–321	1.000	6.00	3.57	10	9
–321	1.000	6.00	3.57	11	9

The results are plotted in Fig. 9. The agreement is fairly good. Note that Ref. [7] does not make clear as to whether $\sigma_y = 81.9$ ksi is the biaxial or uniaxial yield stress. If, however, it represents the biaxial yield stress, then $\sigma^* = 74$ ksi and $k = 58.5$ ksi $\sqrt{\text{in.}}$ and the agreement is even better (see Fig. 10).

(2) Material: 2014-T6 aluminum alloy

σ_Y: 90.8 ksi $\quad\quad \sigma^* = 95.2$ ksi

σ_u: 108.4 ksi $\quad\quad k = 51.7$ ksi $\sqrt{\text{in.}}$

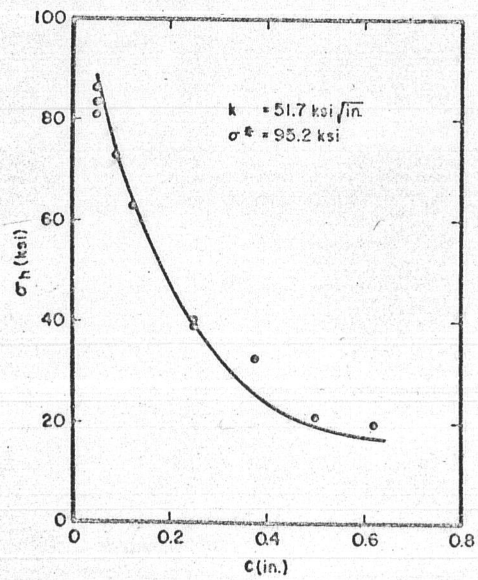

FIG. 11 COMPARISON BETWEEN THEORY AND EXPERIMENT FOR 2014-T6A1 CYLINDRICAL VESSELS AT –423°F

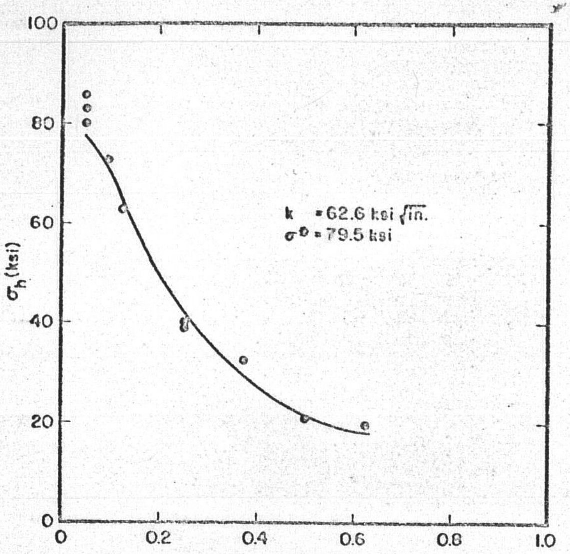

FIG. 12 COMPARISON BETWEEN THEORY AND EXPERIMENT FOR 2014-T6Al CYLINDRICAL VESSELS AT −423°F

T° F	c (in.)	λ	I	σ_h exp. ksi	σ_h calc. ksi
−423	0.050	0.30	1.03	81	89.0
−423	0.050	0.30	1.03	83	89.0
−423	0.050	0.30	1.03	86	89.0
−423	0.075	0.45	1.05	73	76.0
−423	0.125	0.75	1.12	63	64.0
−423	0.250	1.50	1.40	40	39.3
−423	0.250	1.50	1.40	39	39.3
−423	0.375	2.25	1.74	33	26.8
−423	0.500	3.00	2.11	21	19.4
−423	0.625	3.76	2.49	20	17.0

The results are plotted in Fig. 11. The agreement is not very good. Here again the same remark as in part a) holds. Thus, if one uses $\sigma^* = 79.5$ ksi and $k = 62.6$ ksi $\sqrt{\text{in.}}$ the agreement is even better (see Fig. 12).

A. R. Duffy[9] gives results of tests on 30-in. diameter, ⅜-in. thick pipes with through-the-thickness cracks under the following conditions:

Material: X-52 plain carbon (semikilled)

σ_Y: 56 ksi $\sigma^* = 73$ ksi

σ_u: 78 ksi $k = 256$ ksi $\sqrt{\text{in.}}$

T° F	c (in.)	λ	I	σ_h exp. ski	σ_h calc. ksi
29	4.38	3.34	2.29	27.6	25.0
29	2.25	1.72	1.50	46.8	45.4
27	0.50	0.38	1.06	70.6	70.1
30	0.50	0.38	1.06	69.8	70.1
26	1.65	1.26	1.30	55.8	54.2

The results are plotted in Fig. 13. The agreement is good.

Finally Nichols et al.[10] give results of tests on 30-in. diameter, 1-in. thick cylinders with through-the-thickness cracks under the following conditions:

(1) Material: 0.36 C steel

σ_Y: 34.5 ksi $\sigma^* = 43.3$ ksi

σ_u: 69.5 ksi $k = 147.0$ ksi $\sqrt{\text{in.}}$

T° C	c (in.)	λ	I	σ_h exp. ksi	σ_h calc. ksi
1-51°	3.0	0.98	1.20	27.6	31.1
1-51°	3.0	0.98	1.20	32.2	31.1
1-51°	6.0	1.97	1.61	18.8	18.6
1-51°	6.0	1.97	1.61	17.9	18.6
1-51°	6.0	1.97	1.61	21.0	18.6
1-51°	6.0	1.97	1.61	15.9	18.6
1-51°	12.4	4.06	2.63	9.6	8.5

The results are plotted in Fig. 14. The agreement is good. Notice that the scatter of the data points is probably due to the temperature variation.

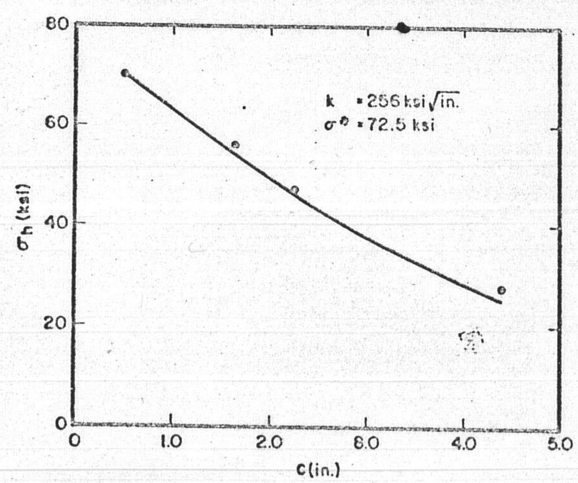

FIG. 13 COMPARISON BETWEEN THEORY AND EXPERIMENT FOR X-52 PLAIN CARBON PIPES

[9] A. R. Duffy, "Studies of Hydrostatic Test Levels and Defect Behavior," *Symposium on Line Pipe Research*, Pipeline Research Committee of American Gas Association, Dallas, Texas, November 17-18, 1965.

[10] R. W. Nichols, W. H. Irvine, A. Quirk, and E. Bevitt, "A Limit Approach to the Presentation of Pressure Vessel Failure," *Proc. First International Conference on Fracture*, Sendai, Japan, 1673, 1966.

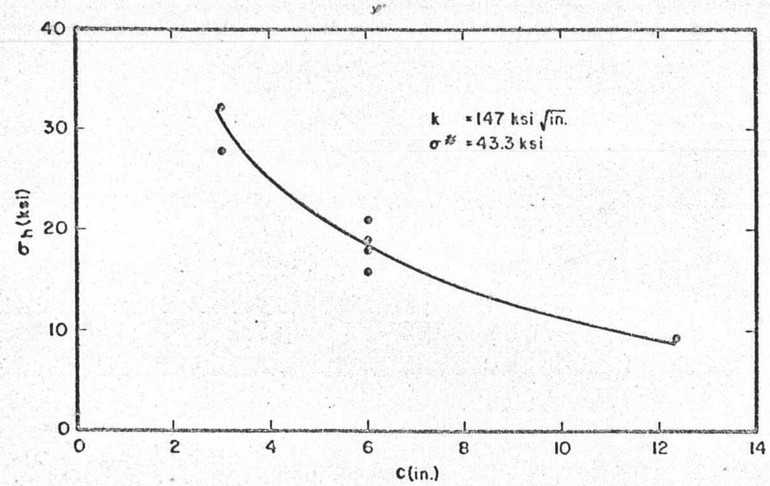

FIG. 14 COMPARISON BETWEEN THEORY AND EXPERIMENT FOR 0.36 C STEEL CYLINDRICAL VESSELS AT 1-51°C

(2) Material: 0.36 C steel

σ_Y: 34.5 ksi $\sigma^* = 43.3$ ksi

σ_u: 69.5 ksi $k = 249.0$ ksi $\sqrt{\text{in.}}$

T° C	c (in.)	λ	I	σ_h exp. ksi	σ_h calc. ksi
62-88	3	0.98	1.20	33.0	35.0
62-88	6	1.97	1.61	25.7	25.0
62-88	6	1.97	1.61	27.7	25.0
62-88	12	3.94	2.57	12.7	13.3
62-88	12	3.94	2.57	15.2	13.3

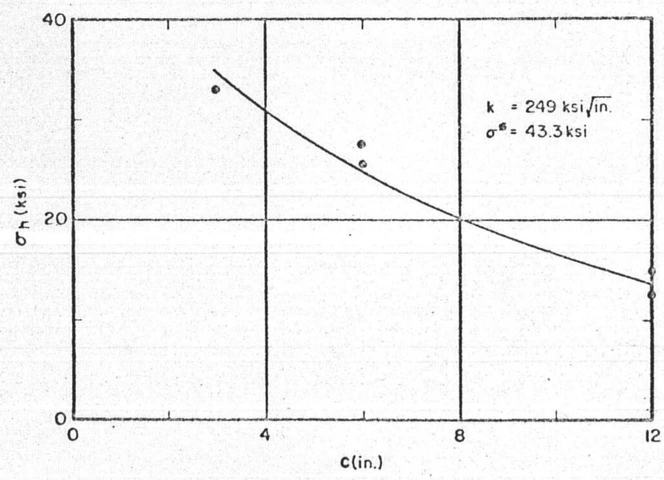

FIG. 15 COMPARISON BETWEEN THEORY AND EXPERIMENT FOR 0.36 C STEEL CYLINDRICAL VESSELS AT 62 TO 88°C

The results are plotted in Fig. 15. The agreement is farily good. There is some temperature variation that affects to some extent, the fracture toughness k.

CONCLUSIONS

The close agreement between the theoretically predicted fracture strengths and the experimental data suggests that Eq. (1) can be used to predict failure in pressurized vessels knowing only the structural geometry, the crack length, the ultimate and yield stresses, and the fracture toughness of the material.

An interesting point, however, should be stressed. It seems from some of the foregoing examples that for very small crack lengths – of the order 1/100 in. – the cosine angle is greater than $\pi/2$ and the criterion, therefore, fails. This failure is due to the fact that the material, at least local to the crack, undergoes considerable strain-hardening; and as a result, the fracture hoop stress is higher than the σ^*. At the present time, there are no adequate criteria to handle this problem. However, the author suggests that for such materials one can use a higher value for σ^* perhaps $\sigma^* = (\sigma_u + \sigma_y)/2$.

This matter properly forms the subject matter for continuing study.

REFERENCES

[1] E. S. Folias, *J. Math. Phys.*, vol. 44, no. 2, June 1965, pp. 164-176, or ARL 64-23, January 1964.

[2] E. S. Folias, *Inter. J. of Fract. Mech.*, vol. 1, no. 2, June 1965, pp. 104-113, or ARL 64-174, October 1964.

[3] E. S. Folias, *Inter. J. of Fract. Mech.*, vol. 3, no. 1, March 1967, pp. 1-11.

[4] E. S. Folias, *Inter. J. of Fract. Mech.*, vol. 1, no. 1, March 1965, pp. 20-46.

[5] E. S. Folias, "On the Effect of Initial Curvature on Cracked Flat Sheets," submitted for publication, *Inter. J. of Fract. Mech.*, January 1969.

[6] E. S. Folias, "On the Theory of Fracture of Curved Sheets," submitted for publication, *Eng. Fract. Mech. J.*, November, 1968.

[7] A. Quirk, "A Maximum Stress Theory for the Failure of Pressure Components Containing Through Thickness Defects," United Kingdom Atomic Energy Authority, AHSB (S)R 134, 1967.

[8] D. S. Dugdale, *J. Mech. Phys. Sol.*, vol. 8, 1960, p. 100.

[9] F. A. McClintock, "On Notch Sensitivity," Welding *J. Res. Suppl.*, vol. 26, 1961, pp. 202, 208.

Appendix

DERIVATION OF EQ. (1)

Following the same analysis as that of Ref. [2], one arrives at the following Griffith-type fracture criterion for initially curved sheets:

$$\frac{(33+6\nu-7\nu^2)(1+\nu)}{3(9-7\nu)}\left[p^{(b)}\right]^2+\left[p^{(e)}\right]^2 \tag{2}$$

$$=\frac{16G\gamma^*}{c\pi}\,\frac{2(1+\nu)}{9-7\nu}\equiv(\sigma_F)^2$$

where the stress coefficients $p^{(b)}$, $p^{(e)}$ are functions of the geometry of the shell and can be found in Refs. [1-5].

However, due to the presence of high stresses in the vicinity of the crack tip, when the appropriate yield criterion is satisfied, then localized plastic deformation occurs and a plastic zone is created. This phenomenon effectively increases the crack length and, therefore, must be accounted for. Following Dugdale [8] the plastic zone size ρ is determined by the relation

$$\frac{c}{\rho+c}=\cos\left(\frac{\pi\sigma}{2\sigma_Y}\right) \tag{3}$$

This relation applies only to a perfect elastic-plastic behavior of a non strain-hardening material. McClintock [9], however, has suggested that a strain-hardening material may be approximated by an ideally plastic one, if a stress higher than σ_y and lower than σ_u is chosen, say σ^*. Thus, correcting the Griffith-Irwin equation so as to include yielding and geometry effect, one has

$$\sigma_F=\frac{2\sigma^*}{\pi}\cos^{-1}\left[\exp\left(-\frac{\pi k^2}{8\sigma^{*2}c}\right)\right] \tag{4}$$

which upon substituting for σ_F from Eq. (2) one obtains Eq. (1).